Journal of Alloys and Compounds 509 (2011) 585–589

Contents lists available at ScienceDirect

Journal of Alloys and Compounds

journal homepage: www.elsevier.com/locate/jallcom

A facile co-gelation route to synthesize FeCo/carbon nanocomposites and their application as magnetically separable adsorber

Zhongli Wang[a,b], Xiaojuan Liu[a], Minfeng Lv[a], Kuiyue Yang[a], Jian Meng[a,*]

[a] State Key Laboratory of Rare Earth Resource Utilization, Changchun Institute of Applied Chemistry, Chinese Academy of Sciences, Changchun 130022, PR China
[b] Graduate University of Chinese Academy of Sciences, Beijing 100049, PR China

ARTICLE INFO

Article history:
Received 12 July 2010
Accepted 20 September 2010
Available online 25 September 2010

Keywords:
Co-gelation sol–gel
Magnetic porous nanocomposite
Adsorption of bulk dyes

ABSTRACT

A new kind of magnetic porous FeCo/carbon nanocomposites was successfully synthesized by using a facile co-gelation sol–gel route. The sol–gel process of this route started from an ethanol solution containing teraethylorthosilicate (TEOS), furfuryl alcohol (FA), and metal nitrates. With the evaporation of solvent, the weak acidity produced from hydrolysis of metal nitrates simultaneously catalyzed the polymerization of FA and the hydrolysis of TEOS, which led to the inorganic/organic hybrid xerogel, accompanying metal salts spontaneously captured in the xerogel. The composites obtained have high surface areas, pore volumes and strong magnetic strengths, which make them exhibit excellent performance of adsorption for bulk dyes and easily separated from solution by external field after adsorption. Compared to the previous methods, this route is very simple and operable for the preparation of magnetic porous carbon composites. Such facile co-gelation route also provides a common path to the synthesis of nanoscale metal or alloy embedded in the porous carbon materials.

1. Introduction

The effluents from textile plants contain portions of dyes, which are deeply colored, multicomponent, and low biodegradable, and have become one of the most serious pollutants in water [1]. For example, most dyes have high tinctorial value, and less than 1 ppm of the dye produces an obvious coloration in water. Many methods have been developed for the removal of dyes, including adsorption, chemical coagulation, photodegradation, biodegradation, active sludge, etc. Among them, adsorption on porous carbons is one of the most efficient processes for dye removal and decoloration, because of large specific surface areas, pore volumes, chemical inertness, and good mechanical stability of carbon. There has been an increasingly large amount of the literature devoted to the study of adsorption for the removal of aqueous-organic species using activated carbon. However, the small particle sizes of activated carbon often cause difficulties when trying to separate activated carbon in liquid–solid phase processes. At present, magnetic separation technology has been paid more and more attention due to the fact that it can be easily separated under an applied magnetic field. Recently, a series of magnetic composite materials have been successfully synthesized and used in many applications. So far, magnetic porous carbon composites have been focus on two kinds of components containing iron oxide/carbon [2–9] and single metal (Fe, Co or Ni)/carbon [10–15]. For example, Dong et al. reported mesostructured γ-Fe_2O_3/carbon composites synthesized by a new cocasting method [3] and Lu et al. fabricated magnetic CMK-3 by deposition Co nanoparticles on the outer surface of a carbon/SBA-15 composite [10].

Fe-Co alloys have exceptional magnetic properties and they exhibit high saturation magnetization, low coercivity, high curie temperature and large magnetic induction. Recently, Fe–Co alloy nanoparticles have been a subject of research for their unique physical, chemical, and magnetic properties that differ from those of the bulk materials [16,17]. In this paper, FeCo alloy nanoparticles were successfully introduced into the porous carbon by a facile co-gelation sol–gel route by using three kinds of precursor containing teraethylorthosilicate (TEOS), furfuryl alcohol, and metal nitrates. According to the precursors utilized, the sol–gel process involves two types of gel routes, one of which is based on hydrolysis-condensation of TEOS and the other is organic polymeric gel of poly(furfuryl alcohol) (PFA) within an ethanol solution containing TEOS, FA, and metal nitrates [18]. Compared to the nanocasting route, the advantage of this method is that the formation of silica template and the impregnation of carbon precursor and metal salts were simultaneously carried out in a co-gelation process, which makes the synthesis very simple and eliminates the time-consuming synthesis of the silica template and multi-steps impregnation process. The porous carbon composites have large surface areas and high saturation magnetizations.

* Corresponding author at: State Key Laboratory of Rare Earth Resource Utilization, Changchun Institute of Applied Chemistry, Chinese Academy of Sciences, Changchun 130022, PR China.
E-mail address: jmeng@ciac.jl.cn (J. Meng).

0925-8388/$ – see front matter © 2010 Elsevier B.V. All rights reserved.
doi:10.1016/j.jallcom.2010.09.101

Different amounts of alloy loading lead to different pore features and magnetic properties. More importantly, the nanocomposites were successfully applied to removal of dyes from water as efficient magnetically separable adsober.

2. Experimental

2.1. Synthesis of magnetic porous carbon composites

Magnetic porous carbon materials were prepared by co-gelation of furfuryl alcohol, metal nitrates and teraethylorthosilicate at 40 °C and 80 °C, followed by a carbonization treatment at 900 °C under inert gas and removing silica in hot NaOH solution. In a typical preparation, 1 mmol metal nitrates (0.5 mmol $Fe(NO_3)_3{\cdot}9H_2O$ and 0.5 mmol $Co(NO_3)_2{\cdot}6H_2O$) was dissolved in 1 ml ethanol, followed by mixing with 1 g furfuryl alcohol. After stirring for 15 min, 2 g TEOS was added into the mixture. After stirring for another 30 min, the red solution obtained was transferred into dishes. It took 12 h at 40 °C and 8 h at 80 °C in an open system of water bath for the thermopolymerization and sol–gel process. Usually, HCl solution was added to the TEOS solution before adding the carbon precursor in order to pre-hydrolyze the silica precursor solution. In contrast, metal nitrates solution instead of HCl solution provides weak acid media, especially for the iron nitrate solution. With the ethanol evaporating and the solution contacting, the acidity gradually increased and the simultaneous polymerization was initiated. The xerogel obtained was carbonized at 900 °C for 2 h with a ramping rate of 2 °C/min under nitrogen flow. Then the silica in the composite was removed by washing with heated 1 M NaOH solution. The final product was denoted as FeCo/C-1. The same procedures were carried out for the preparation of samples FeCo/C-1.5 and FeCo/C-2, except that the amounts of metal nitrates were 1.5 mmol and 2 mmol, keeping the molar ration of $Fe(NO_3)_3{\cdot}9H_2O$ and $Co(NO_3)_2{\cdot}6H_2O$ to 1:1, for FeCo/C-1.5 and FeCo/C-2, respectively.

2.2. Adsorption of dyes

Dyes solution (0.4 g/L) was prepared by dissolving 0.1 g of dye in 250 ml distilled water. In a typical adsorption experiment, 50 mg of porous composite adsorbent was suspended in 50 ml of dye solution. The resulting mixture was kept under mechanical stirring for 12 h at room temperature. The adsorption amount of dyes was measured by standard UV/Vis adsorption method. Magnetic separation of the nanocomposite prior to the analysis was used to avoid potential interference from suspended scattering particles in the UV/Vis analysis.

2.3. Characterization and measurement

Wide-angle X-ray diffraction (XRD) patterns were collected on Bruker D8 Smart APPEX II X-ray diffractometer using Cu Kα radiation (40 kV, 40 mA). The energy-dispersive X-ray (EDX) spectra were performed by using a field emission scanning electron microscopy (FE-SEM, HITACHI S-4800). Transmission electron microscopy (TEM) images were taken on a FEI Tacnai G2 electron microscope operated at 200 kV. For TEM measurements, the samples were prepared by dispersing the powder products as slurry in ethanol and drying on a holey carbon film on a Cu grid for measurements. N_2 adsorption–desorption isotherms were measured with a Micromeritics 2010 analyzer at 77 K. Before measurements, the samples were degassed at 150 °C for more than 5 h. The Brunauer–Emmett–Teller (BET) method was utilized to calculate the specific surface areas. The pore size distributions were derived from the desorption branches of the isotherms based on the Barrett–Joyner–Halanda (BJH) model. The total pore volume was estimated from the amount adsorbed at a relative pressure (P/P_0) of 0.99. The magnetic properties of the samples were investigated by superconducting quantum interference device (SQUID) magnetometer at 300 K.

3. Results and discussion

The synthetic procedure for the porous magnetic FeCo/carbon composites is illustrated in Scheme 1. There are three steps in the preparation process including co-gelation, carbonization and NaOH etching. The sol–gel process of this route started from an ethanol solution containing TEOS, FA, and metal nitrates. With the evaporation of solvent, the weak acidity produced from hydrolysis of metal nitrates simultaneously catalyzed the polymerization of furfuryl alcohol (FA) and the hydrolysis of teraethylorthosilicate (TEOS), which led to the inorganic/organic hybrid xerogel, accompanying metal salts spontaneously captured in the xerogel. Homogeneous black xerogels are formed after co-gelation sol–gel process of step 1. During the carbonization of step 2, polyfurfuryl alcohol was transferred into carbon through deoxidation and dehydrogenation reactions, meanwhile metal nitrates were decomposed and then in situ reduced by the carbon. From the analysis of EDX mapping (Fig. S1), it can be seen that all the elements (C, Si, Fe, Co, O) in the composites were almost uniformly distributed, indicating the homogenization of the xerogel. In step 3, the final porous composites were obtained after washing the silica framework, a hard template, in hot NaOH solution.

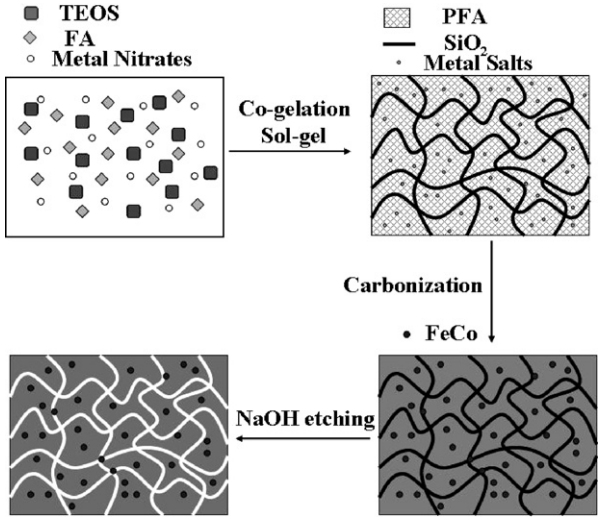

Scheme 1. Illustration of the synthesis process.

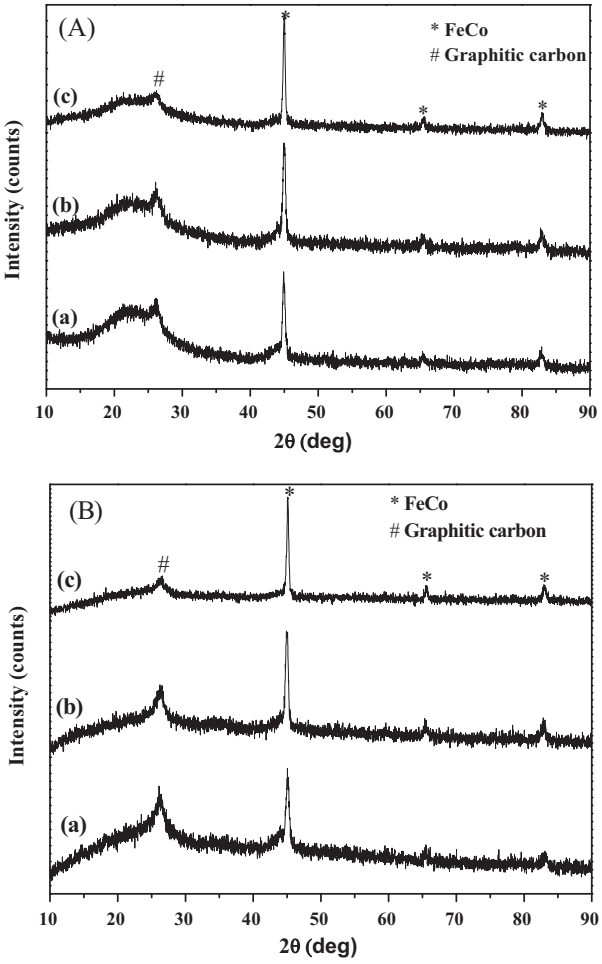

Fig. 1. XRD patterns of nanocomposites before (A) and after (B) removal of silica: (a) FeCo/C-1, (b) FeCo/C-1.5, and (c) FeCo/C-2, respectively.

Table 1
FeCo contents, pore structure parameters, saturation magnetization and adsorption capacity of nanocomposites.

Sample	FeCo content (wt%)	Surface area (m^2/g)	Pore volume (cm^3/g)	Micropore volume (cm^3/g)	Pore size (nm)	Saturation magnetization (emu/g)	Adsorption capacity (mg/g)		
							MBT	RB	MO
FeCo/C-1	8.6	653.5	0.55	0.20	4, 6	9.5	253	239	152
FeCo/C-1.5	12.5	481.4	0.48	0.13	4, 8	17.8	210	195	129
FeCo/C-2	16.2	381.6	0.38	0.10	4, 9	22.2	177	155	99

The composite products after carbonization were characterized by XRD patterns shown in Fig. 1A. There are three resolved diffraction peaks of FeCo alloy, which can be assigned to 1 1 0, 2 0 0 and 2 1 1 reflections according to the JCPDS Card Number 49-1567. One peak of graphite carbon at 26° and the wide peak of amorphous silica at around 22° were also obvious observed. Except for the above diffraction peaks mentioned, no other peaks of impurities were observed in the products after carbonization, indicating that even though there were some possible products such as metal carbides or silicates, the amount of them was very little. Furthermore, the formation of alloy improved the stability of metal, for example, in the single metal Fe/carbon composite, impurity was observed (Fig. S2). After etching in hot NaOH solution, the amorphous peaks of silica disappeared and the peaks of graphite were clearly shown (Fig. 1B). During the long-time dealing process of basic media, there were no changes for diffraction peaks of FeCo alloy, indicating the stability of alloy in the basic solution. With increasing content of metal salts, the peaks of alloy become stronger and sharper, indicating the increase of the amount and sizes of the alloy particles. This trend is further illustrated by the change of diffraction intensity of alloy with content as shown in Fig. 2. The contents of FeCo alloy in the composite were measured by EDX spectroscopy analysis, which are listed in Table 1.

Fig. 3a–c shows the TEM images of the porous FeCo/carbon composites with different alloy contents, which illustrates FeCo nanoparticles uniformly embedded in the carbon matrix. With

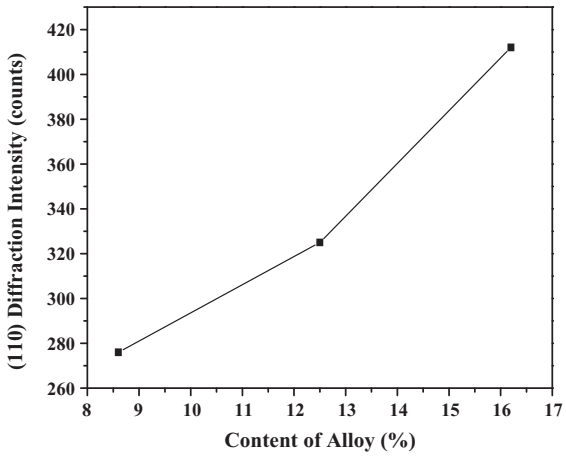

Fig. 2. The change of (1 1 0) diffraction intensity with content of alloy FeCo nanoparticles.

increasing content of metal salts, the distribution of the particles become dense and the sizes become large, which is in agreement with the results of XRD patterns. From the enlarged images of composites (Fig. 3d–f), it was clearly observed that the sizes of particles become larger and larger with alloy content, 20–30 nm for FeCo/C-1, 30–40 nm for FeCo/C-1.5 and 50–60 nm for FeCo/C-2,

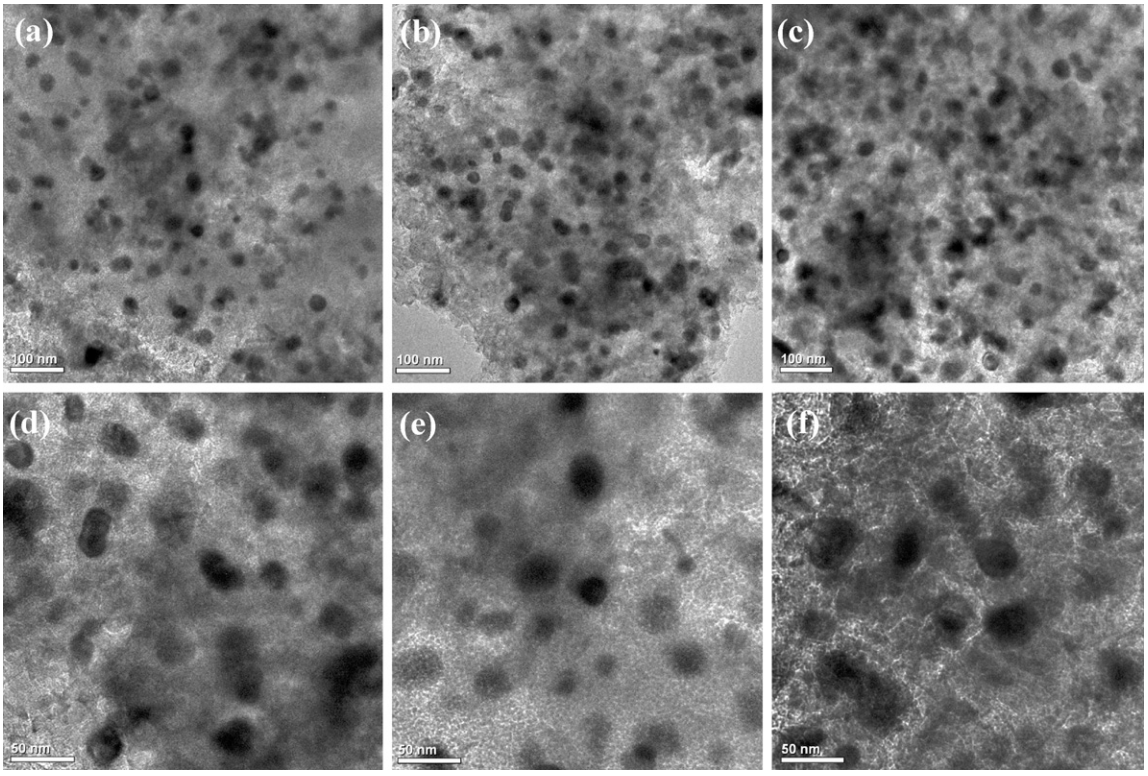

Fig. 3. TEM images of porous FeCo/carbon nanocomposites FeCo/C-1 (a and d), FeCo/C-1.5 (b and e), and FeCo/C-2 (c and f).

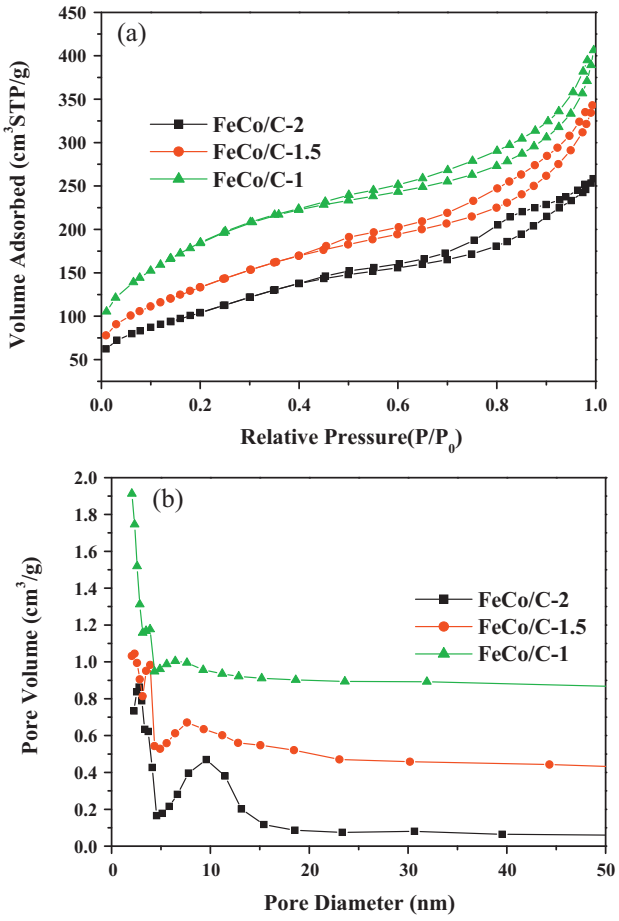

Fig. 4. Nitrogen sorption isotherms (a) and pore size distribution curves (b) of magnetic porous carbon nanocomposites.

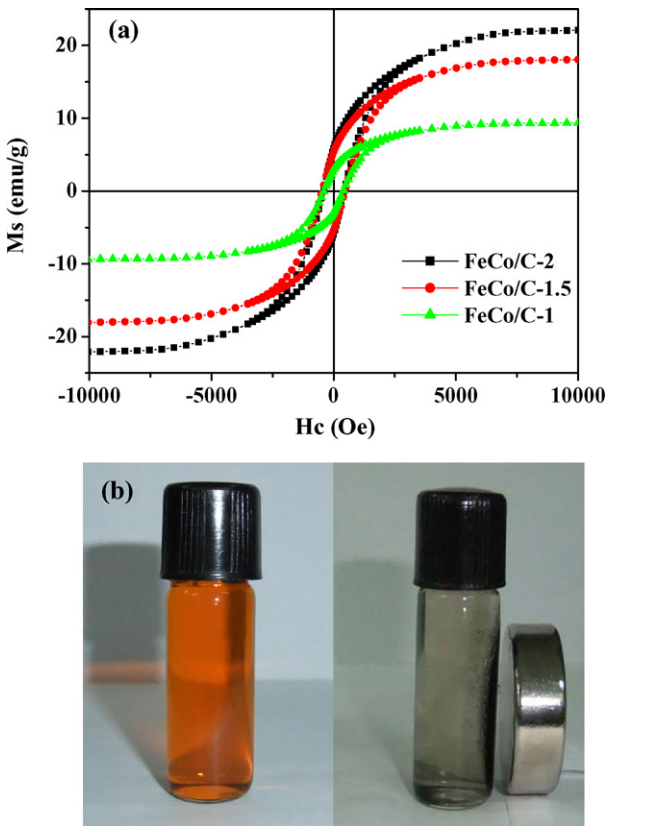

Fig. 5. (a) Magnetization curves of porous FeCo/carbon nanocomposites FeCo/C-1, FeCo/C-1.5, and FeCo/C-2 at room temperature, respectively; (b) magnetic separation from MO solution for Fe_7Co_3/carbon nanocomposites under an external magnet.

respectively. The interstitial porosity of the composites can be also observed from the enlarged TEM images.

Nitrogen sorption isotherms were recorded to investigate the effect of the FeCo content on the pore properties of the samples. Fig. 4 shows the nitrogen sorption isotherms of FeCo/C-1, FeCo/C-1.5, and FeCo/C-2 samples. All the isotherm curves of the samples are found to be of type IV curves. The surface area is found to decrease gradually from FeCoC-1 to FeCo/C-2 with increasing the content of alloy, and similarly, the pore volume decreases also in this order, as shown in Table 1. The main reason for such decrease can be attributed to the presence of a large amount of FeCo particles because of its much higher density than carbon. However, complex pore size distributions of the composites can be found in Fig. 4b and Table 1, including hierarchical micropores and mesopores. The micropore volume calculated from t-plot method decreases with the increase of FeCo content, in accordance with the pore sizes distribution, especially for FeCo/C-1 which has not complete curve of pore size distribution under mesoporous measurement condition. It can also be seen that three composites have two mesopore systems. One pore system centered at around 3.9 nm, common to three samples, which should be created by the dissolution of the silica walls. Another pore system, interestingly, varied with increasing FeCo alloy contents and the pore sizes f 6 nm to 9 nm, which should be formed by the interstitial voids created during the production of alloy, in accordance with the above TEM results.

The magnetic properties were characterized by magnetic hysteresis loops with varying magnetic field at 300 K. As shown in Fig. 5a, three samples exhibit typically soft magnetic features with low coercivity and low remanance. The corresponding saturation magnetization strengths (Ms) are 9.5, 17.8, and 22.2 emu/g, respectively, increasing with the alloy contents. These values are much lower than that of bulk FeCo, which is attributed to the nanosize of the FeCo particles and the presence of carbon.

Removal of weakly biodegradable pollutants such as bulky dyes in water is very important for the protection of our environment [1]. Due to the large specific surface area, pore volume, chemical inertness, and good mechanical stability, adsorption on porous carbon is one of the most efficient processes for dye removal and decoloration. In this paper, methylene blue trihydrate (MBT), rhodamine B (RB) and methyl orange (MO) were chosen to investigate the adsorption capacity of magnetic carbon composite. The molecular size, weight and nature of three dyes are listed in Table S1. The composites exhibit high capacities (as high as 253 mg/g) in adsorbing bulky dyes, regardless of the nature, including acidic (MO), basic (MBT and RB), and azo (MO) dyes, as shown in Table 1. The capacities of porous composites for all the dyes decrease with the increase of alloy loading, similarly to the variation of surface areas and pore volumes, and it suggests that the capacity is influenced by pore structure properties of the adsorbent. The composite was easily attracted to the magnet within a short time after adsorption, which provides an effective way to separate the magnetic composite from suspension (Fig. 5b).

4. Conclusions

In conclusion, by using a facile co-gelation sol–gel method, a new kind of magnetic porous FeCo/carbon composites was successfully synthesized. Such magnetic nanocomposites have high surface areas, large pore volumes and strong magnetization. Application of these composites as efficient magnetically separable

adsorbent was demonstrated in this study. However, one may envisage also other applications, such as a magnetic separable catalyst support. The facile co-gelation route also provides a common path to the synthesis of nanoscale metal or alloy embedded in the porous carbon materials.

Acknowledgements

This project was supported by National Natural Science Foundation of China (Grant No. 20831004 and 20771100).

Appendix A. Supplementary data

Supplementary data associated with this article can be found in the online version, at doi:10.1016/j.jallcom.2010.09.101.

References

[1] X. Zhuang, Y. Wan, C.M. Feng, Y. Shen, D.Y. Zhao, Chem. Mater. 21 (2009) 706–716.
[2] Y.P. Zhai, Y.Q. Dou, X.X. Liu, B. Tu, D.Y. Zhao, J. Mater. Chem. 19 (2009), pp. 3992–3000.
[3] X.P. Dong, H.R. Chen, W.R. Zhao, X. Li, J.L. Shi, Chem. Mater. 19 (2007) 3484–3490.
[4] J. Lee, S. Jin, Y. Hwang, J.G. Park, H.M. Park, T. Hyeon, Carbon 43 (2005) 2536–2543.
[5] A.B. Fuertes, P. Tartaj, Chem. Mater. 18 (2006) 1675–1679.
[6] A.B. Fuertes, T. Valdeĩs-Soliĩs, M. Sevilla, J. Phys. Chem. C 112 (2008) 3648–3654.
[7] N. Yang, S.M. Zhu, D. Zhang, S. Xu, Mater. Lett. 62 (2008) 645–647.
[8] H.M. Cao, G.J. Huang, S.F. Xuan, Q.F. Wu, F. Gu, C.Z. Li, J. Alloys. Compd. 448 (2008) 272–276.
[9] L.Y. Chen, Z.X. Xu, H. Dai, S.T. Zhang, J. Alloys. Compd. 497 (2010) 221–227.
[10] A.H. Lu, W. Schmidt, N. Matoussevitch, H. Bonnemann, B. Spliethoff, B. Tesche, F. Schuth, Angew. Chem. Int. Ed. 43 (2004) 4303–4306.
[11] I.S. Park, M. Choi, T.W. Kim, R. Ryoo, J. Mater. Chem. 16 (2006) 3409–3416.
[12] M. Schwickardi, S. Olejnik, E.L. Salabas, W. Schmidt, F. Schuth, Chem. Commun. (2006) 3987–3989.
[13] D.W. Wang, F. Li, G.Q. Lu, H.M. Cheng, Carbon 46 (2008) 1593–1599.
[14] M. Sevilla, P. Valle-Vigon, P. Tartaj, A.B. Fuertes, Carbon 47 (2009) 2519–2527.
[15] Y.F. Zhu, E. Kockrick, S. Kaskel, T. Ikoma, N. Hanagata, J. Phys. Chem. C 113 (2009) 5998–6002.
[16] Z.L. Wang, X.J. Liu, M.F. Lv, J. Meng, Mater. Lett. 64 (2010) 1219–1221.
[17] D. Carta, G. Mountjoy, M. Gass, G. Navarra, M.F. Casula, A. Corrias, J. Chem. Phys. 127 (2007) 204705.
[18] M. Kakihana, J. Sol.–Gel Sci. Technol. 5 (1996) 7–55.